

VENDOR'S DOCUMENT REVIEW	
1	<input checked="" type="checkbox"/> APPROVED - MANUFACTURING MAY PROCEED
2	<input type="checkbox"/> APPROVED - SUBMIT FINAL DOCUMENT - MANUFACTURING MAY PROCEED
3	<input type="checkbox"/> APPROVED AS NOTED - MAKE CHANGES AND SUBMIT FINAL DOCUMENT - MANUFACTURING MAY PROCEED AS APPROVED
4	<input type="checkbox"/> NOT APPROVED - CORRECT AND RESUBMIT
5	<input type="checkbox"/> REVIEW NOT REQUIRED - MANUFACTURING MAY PROCEED

APPROVAL OF THIS DOCUMENT DOES NOT RELIEVE SUPPLIER FROM FULL COMPLIANCE WITH CONTRACT OR PURCHASE ORDER REQUIREMENTS

BY: [Signature] DATE: 10/15/97
 ROCHESTER GAS & ELECTRIC CORP.
 ROCHESTER, NY

Report No.: SIR-97-077
 Revision No.: 0
 Project No.: RGE-07Q
 File No.: RGE-07Q-401
 August 1997

**Leak-Before-Break Evaluation of Portions
 of the Residual Heat Removal (RHR) System
 at R. E. Ginna Nuclear Power Station**

Prepared for:

Rochester Gas & Electric Corporation

Prepared by:

Structural Integrity Associates, Inc.
 San Jose, California

Prepared by: [Signature]
 C. C. Markovits

Date: 8/29/97

Reviewed by: [Signature]
 A. F. Deardorff

Date: 8/29/97

*Reviewed and
 Approved by:* [Signature]
 N. G. Cofie

Date: 8/29/97



EXECUTIVE SUMMARY

The residual heat removal system (RHR) at R. E. Ginna Nuclear Power Station was evaluated for leak-before-break (LBB) behavior in accordance with the NRC GDC-4 and NUREG-1061, Vol. 3. The RHR lines considered in this evaluation are adjacent to the hot and cold legs of the reactor coolant system (RCS). They are 10-inch Schedule 160 piping, fabricated from Type 316 stainless steel. The operating pressure for the RHR lines is 2235 psig and the operating temperature was conservatively chosen as 612.2°F for the evaluation.

LBB was demonstrated for the above piping in accordance with NRC margins. In this evaluation, circumferential flaws were considered since these are more limiting than axial flaws. The evaluation consisted of determining critical flaw sizes at selected locations on the piping in the vicinity of the Component Cooling Water (CCW) piping to the reactor support coolers. The critical flaw sizes were calculated using the elastic-plastic fracture mechanics (EPFM) J-Integral/Tearing Modulus (J/T) approach. Leakages were then calculated through half the critical flaw sizes per the requirements of NUREG-1061. The leakage evaluation was done for the affected nodal locations in the piping mathematical models provided by Rochester Gas & Electric Corporation (RG&E).

The predicted leakage for all the locations on the RHR lines considered in evaluation was at least 4.7 gpm considering the required NRC safety factor of 2 between the critical flaw size and the leakage flaw size. This leakage should be easily detected by the present leak detection system at Ginna.

A fatigue crack growth analysis was performed to study the predicted behavior of postulated semi-elliptical, inside surface flaws. Postulated circumferential flaws of 15% of the pipe wall in depth, and with an aspect ratio (length to depth) equal to or larger than 10, were shown to grow an insignificant amount in depth and length during 40 years. The above postulated flaw sizes are slightly in excess of the maximum size permitted by ASME Code, Section XI, IWB-3514, and are conservative since such flaws would have been repaired during the preservice inspection.

Postulated flaws deeper than 15% of the wall were also studied, and shown to grow preferentially



through the pipe wall and result in leakage, rather than to extend an unacceptable amount in length. This result further validates the application of LBB methodology to the prevention of pipe rupture for this system.

The effect of degradation mechanisms which could impact the LBB evaluations were considered in the evaluation. It was determined that the probability of water hammer occurrence in the affected portions of RHR piping is very low. In addition, RG&E has utilized EPRI guidelines and research results to prevent or mitigate water hammer in Ginna systems. Corrosion is not an expected failure mechanism for the system evaluated based on plant experience and RG&E's continuing erosion-corrosion monitoring program.

Table of Contents

<u>Section</u>	<u>Page</u>
1.0 INTRODUCTION	1-1
1.1 Background.....	1-1
1.2 Leak-Before-Break Methodology	1-1
2.0 CRITERIA FOR APPLICATION OF LEAK-BEFORE-BREAK APPROACH.....	2-1
2.1 Criteria for Through-Wall Flaws	2-1
2.2 Criteria for Part-Through-Wall Flaws	2-2
2.3 Other Mechanisms.....	2-2
3.0 CONSIDERATION OF WATER HAMMER, CORROSION AND FATIGUE.....	3-1
3.1 Water Hammer	3-1
3.2 Corrosion	3-1
3.3 Fatigue	3-2
4.0 PIPING MATERIALS AND STRESSES	4-1
4.1 Piping System Description.....	4-1
4.2 Material Properties	4-1
4.3 Piping Stresses.....	4-2
5.0 LEAK-BEFORE-BREAK EVALUATION	5-1
5.1 Evaluation of Critical Flaw Sizes.....	5-1
5.2 Leak Rate Determination	5-3
5.3 LBB Evaluation Results and Discussions.....	5-8
6.0 EVALUATION OF FATIGUE CRACK GROWTH OF SURFACE FLAWS.....	6-1
7.0 SUMMARY AND CONCLUSIONS	7-1
8.0 REFERENCES	8-1





List of Tables

<u>Table</u>	<u>Page</u>
Table 4-1 Material Constants Used for Type 316 Stainless Steel in LBB Evaluation	4-3
Table 4-2 Calculation of Stresses for RHR Pipe Run from Valve 700 to Hot Leg	4-4
Table 4-3 Calculation of Stresses for RHR Pipe Run from Valve 721 to Cold Leg	4-5
Table 5-1 Summary of Critical Flaw Sizes	5-9
Table 5-2 LBB Evaluation Results for Detectable Leakage	5-10
Table 6-1. Plant Design Transients for RHR Piping	6-5
Table 6-2. Combined Transients For Fatigue Crack Growth Evaluation For RHR Line Adjacent to Hot Leg	6-6
Table 6-3 Combined Transients For Fatigue Crack Growth Evaluation For RHR Line Adjacent to Cold Leg	6-7
Table 6-4 Combined Maximum and Minimum Stresses for Fatigue Growth Analysis for RHR Line Adjacent to Hot Leg	6-8
Table 6-5 Combined Maximum and Minimum Stresses for Fatigue Crack Growth Analysis for RHR Line Adjacent to Cold Leg	6-9
Table 6-6 Results of Fatigue Crack Growth	6-10



List of Figures

<u>Figure</u>	<u>Page</u>
Figure 1-1. Location of RHR Line Adjacent to the Hot Leg.....	1-4
Figure 1-2. Location of the RHR Line Adjacent to the Cold Leg (Part A)	1-5
Figure 1-3. Location of the RHR Line Adjacent to the Cold Leg (Part B)	1-6
Figure 1-4. Representation of Postulated Cracks in Pipes for FractureMechanics Leak-Before-Break Analysis	1-7
Figure 1-5. Illustration of ISI (UT)/Leak Detection Approach to Protection Against Pipe Rupture.....	1-8
Figure 1-6. Leak-Before-Break Approach Based on Fracture Mechanics Analysis with In-service Inspection and Leak Detection	1-9
Figure 5-1. Flow of Subcooled Water Through a Crack.....	5-11
Figure 5-2. Leak Rate Versus Crack Size for RHR Pipe Run from Valve 700 to Hot Leg	5-12
Figure 5-3. Leak Rate Versus Crack Size for RHR Pipe Run from Valve 721 to Cold Leg	5-13

1.0 INTRODUCTION

1.1 Background

This report documents evaluations performed by Structural Integrity Associates (SI) to determine the leak-before-break (LBB) capabilities of several locations on the residual heat removal (RHR) System at R. E. Ginna Nuclear Power Station (Ginna). These evaluations are necessary because a pipe break at these locations could potentially affect the structural integrity of Component Cooling Water (CCW) piping to the reactor support coolers per Reference 29.

Two portions of the RHR line are considered in the evaluation and are shown in Figures 1-1 through 1-3 [1]. The first portion includes the piping from the hot leg of the reactor coolant system (RCS) to motor operated valve (MOV) 700 (Node points 680 through 70 in Figure 1-1). The second portion extends from the RCS cold leg to MOV 721 (Nodes points 960 through 8400 in Figures 1-2 and 1-3).

1.2 Leak-Before-Break Methodology

NRC SECY-87-213 [2] covers a final broad scope rule to modify General Design Criterion 4 (GDC-4) of Appendix A, 10 CFR Part 50. This amendment to GDC-4 allows exclusion from the design basis of dynamic effects associated with high energy pipe rupture by application of LBB technology.

Definition of the LBB approach and criteria for its use are provided in NUREG-1061 [3]. Volume 3 of NUREG-1061 defines LBB as "...the application of fracture mechanics technology to demonstrate that high energy fluid piping is very unlikely to experience double-ended ruptures or their equivalent as longitudinal or diagonal splits." The particular crack types of interest include circumferential through-wall cracks (TWC) and part-through-wall cracks (PTWC), as well as axial or longitudinal through-wall cracks (TWC), as shown in Figure 1-4.



LBB is based on a combination of in-service inspection (ISI) and leak detection to detect cracks, coupled with fracture mechanics analysis to show that pipe rupture will not occur for cracks smaller than those detectable by these methods. A discussion of the criteria for application of LBB is presented in Section 2 of this report, which summarizes the NUREG-1061 requirements.

The approach to LBB which has gained acceptance for demonstrating protection against high energy line break (HELB) in safety-related nuclear piping systems is schematically illustrated in Figure 1-5. Essential elements of this technique include critical flaw size evaluation, crack propagation analysis, volumetric nondestructive examination (NDE) for flaw detection/sizing, leak detection, and service experience. In Figure 1-5, a limiting circumferential crack is modeled as having both a short through-wall component, and an axisymmetric part-through-wall crack component. Leak detection establishes an upper bound for the through-wall crack component while volumetric ISI limits the size of undetected part-through-wall defects. These detection methods complement each other, since volumetric ISI techniques are well suited to the detection of long cracks while leakage monitoring is effective in detecting short through-wall cracks. The level of ISI required to support LBB involves volumetric inspection at intervals determined by fracture mechanics crack growth analysis, which would preclude the growth of detectable part-through-wall cracks to a critical size during an inspection interval. The objective of this fatigue evaluation is to limit potentially undetected defect sizes to those which would be allowed under ASME Section XI rules. For through-wall defects, crack opening areas and resultant leak rates are compared with leak detection limits.

The net effect of complementary leak detection and ISI is shown by the shaded region of Figure 1-5 as the largest undetected defect that can exist in the piping at any given time. Critical flaw size evaluation, based on elastic-plastic fracture mechanics techniques, is used to determine the length and depth of defects that would be predicted to cause pipe rupture under specific design basis loading conditions, including abnormal conditions such as a seismic event and including appropriate safety margins for each loading condition. Crack propagation analysis is used to determine the time interval in which the largest undetected crack could grow to a size which would impact plant safety margins. A summary of the elements for a leak-before-break analysis is shown



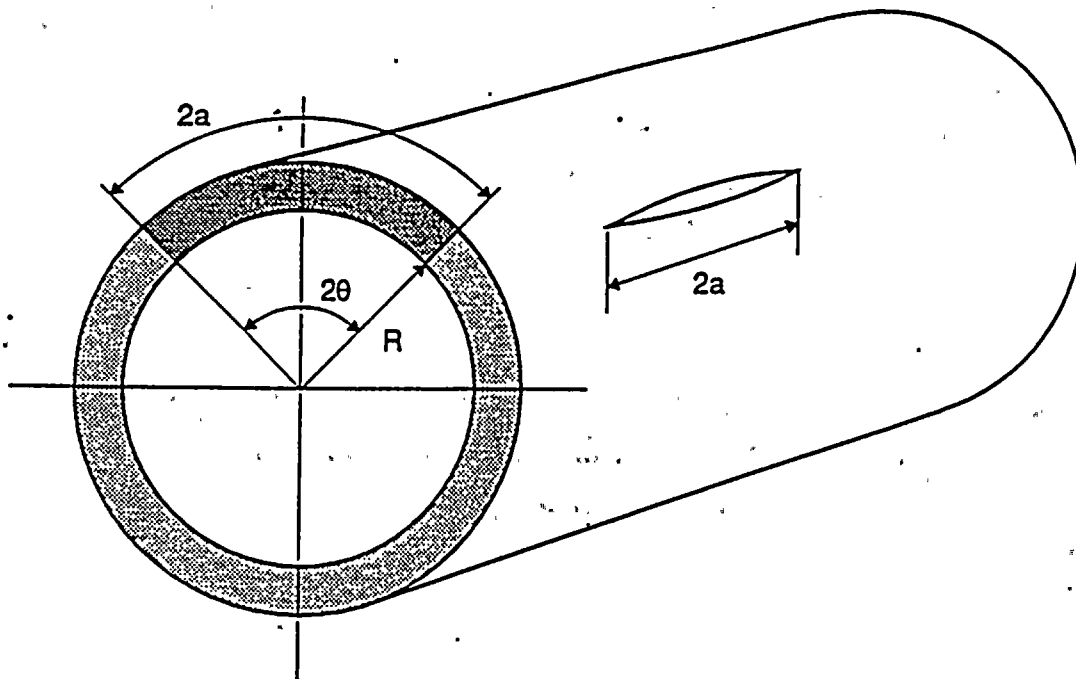
in Figure 1-6. Service experience, where available, is useful to confirm analytical predictions as well as to verify that such cracking tends to develop into "leak" as opposed to "break" geometries.

In accordance with NUREG-1061, Volume 3 [3] and other NRC guidance on the topic, the leak-before-break technique for high energy piping systems in a nuclear power plant should include the following considerations.

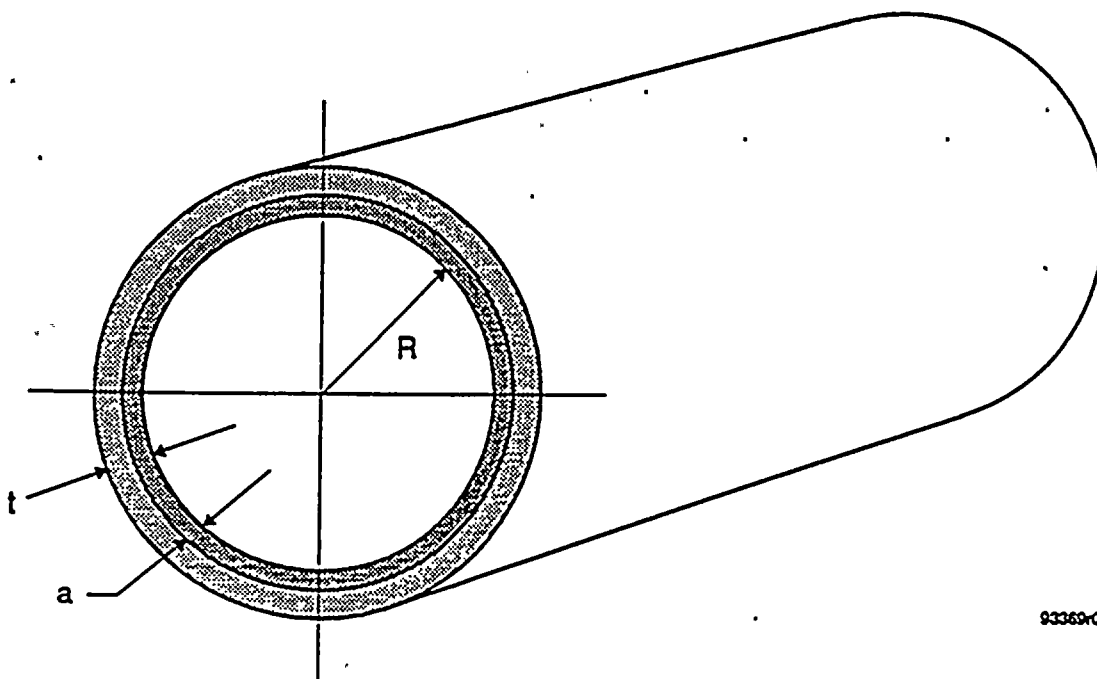
- Elastic-plastic fracture mechanics analysis of load carrying capacity of cracked pipes under worst case normal loading, with safe-shutdown earthquake (SSE) loads included. Such analysis should include recent elastic-plastic fracture data applicable to pipe weldments and weld heat affected zones where appropriate.
- Consideration of pipes under limit load conditions for the piping system, as applicable.
- Linear elastic fracture mechanics analysis of subcritical crack propagation to determine ISI (in-service inspection) intervals for long, part-through-wall cracks.

Piping stresses have a dual role in LBB evaluations. On one hand, higher maximum (design basis) stresses tend to yield lower critical flaw sizes, which result in smaller flaws for leakage and a lower leakage rate. On the other hand, higher operating stresses tend to open cracks more for a given crack size and create a higher leakage rate. Because of this duality, the use of a single maximum stress location for a piping system may result in a non-conservative LBB evaluation. This LBB evaluation will, therefore, be performed in such a manner that the affected nodal locations for the piping models of the RHR lines will be specifically addressed.





a. Circumferential and Longitudinal Through-Wall Cracks of Length $2a$.



b. Circumferential 360° Part-Through-Wall Crack of Depth a .

Figure 1-4. Representation of Postulated Cracks in Pipes for Fracture Mechanics Leak-Before-Break Analysis

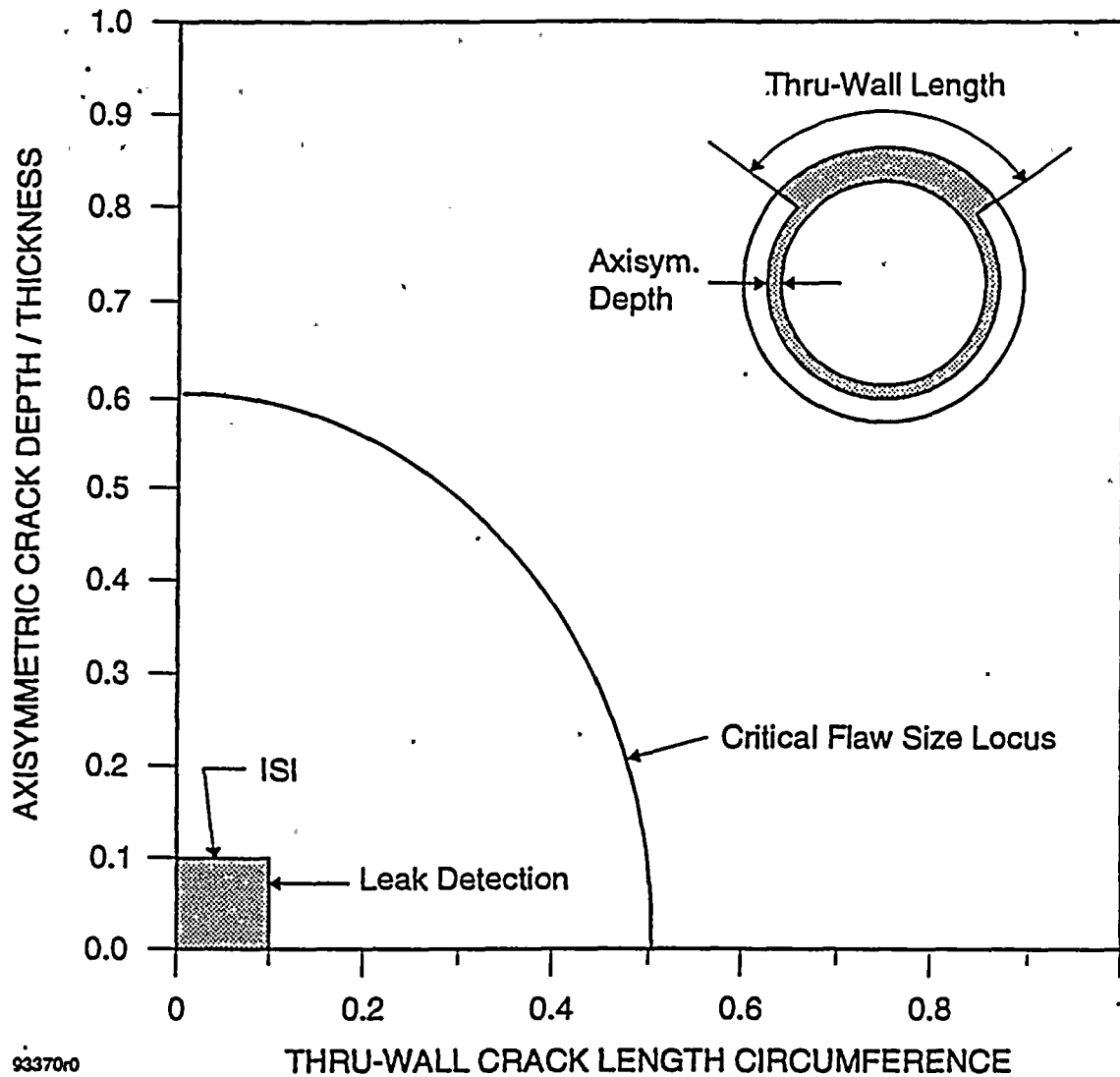
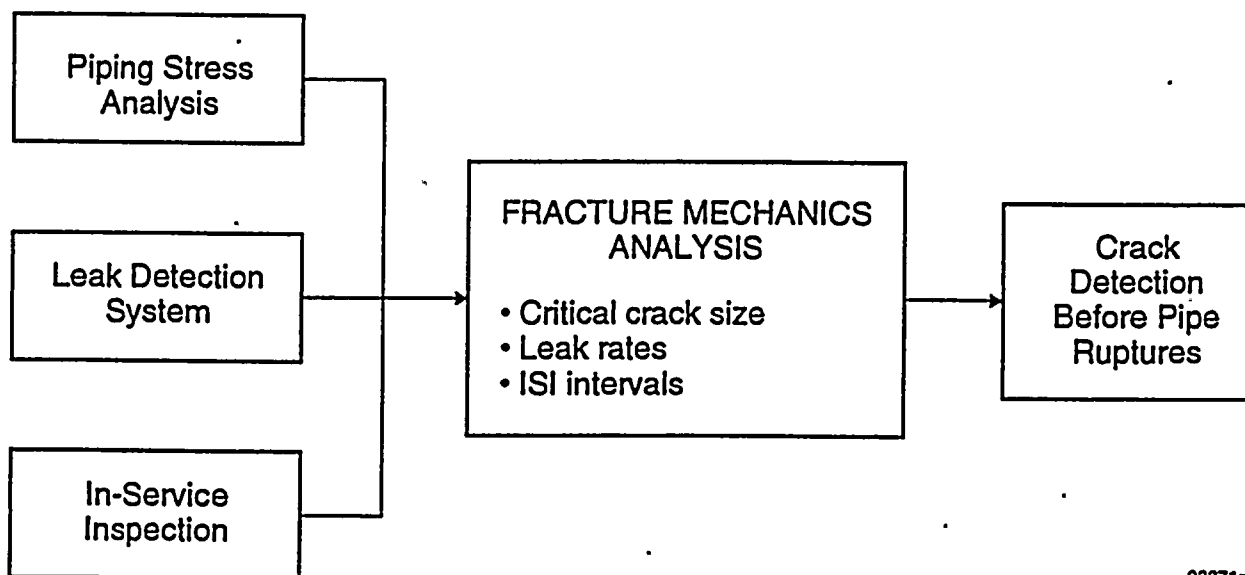


Figure 1-5. Illustration of ISI (UT)/Leak Detection Approach to Protection Against Pipe Rupture



93371r0

Figure 1-6. Leak-Before-Break Approach Based on Fracture Mechanics Analysis with In-service Inspection and Leak Detection

2.0 CRITERIA FOR APPLICATION OF LEAK-BEFORE-BREAK APPROACH

NUREG-1061, Volume 3 [3] and GDC-4 (SRP 3.6.3) [2] identify several criteria to be considered in determining applicability of the leak-before-break approach to piping systems.

Section 5.2 of Reference 3 provides an extensive discussion of the criteria for performing leak-before-break analyses. The details of that discussion will not be repeated here, but a summary of various requirements as applied to evaluation of the RHR line at Ginna is provided below.

2.1 Criteria for Through-Wall Flaws

Acceptance criteria for critical stresses and critical flaws are:

1. The flaw which is required to produce an "acceptable leakage rate" is smaller than the critical flaw length associated with the maximum stress (with SSE) by a factor of 2.
2. The stress required to make the "acceptable leakage rate" flaw critical is greater than the maximum stress (with SSE) by a factor of at least $\sqrt{2}$.
3. The net section collapse criterion (NSCC) approach may be used to compute the critical flaw size provided a safety factor of 3 is placed on normal service stresses.

It has been found in previous LBB evaluations conducted by Structural Integrity Associates (SI), that the second and third criteria stated above are not bounding. The method described in the first criteria provides a smaller leakage rate than the second criteria as was demonstrated in the LBB evaluation previously performed for high energy lines outside containment at Ginna [4]. Therefore, only the first criteria will be considered in this report. Furthermore, the elastic-plastic fracture mechanics (EPFM) approach is generally conservative relative to the NSCC approach when applied to ferritic piping. Therefore, only EPFM principles will be applied in this evaluation.



2.2 Criteria for Part-Through-Wall Flaws

NUREG-1061, Volume 3 [3] requires demonstration that a long part-through-wall flaw which is detectable by ultrasonic means will not grow due to fatigue to a depth which would produce instability over the life of the plant. This is demonstrated in a later section of this report, where the analysis of subcritical crack growth is discussed.

2.3 Other Mechanisms

NUREG-1061, Volume 3 [3] and GDC-4 [2] limit applicability of the leak-before-break approach to those locations where degradation or failure by mechanisms such as water hammer, erosion/corrosion, fatigue, and intergranular stress corrosion cracking (IGSCC) is not a significant possibility. These mechanisms were considered for the RHR line at Ginna, as reported in Section 3 of this report.



3.0 CONSIDERATION OF WATER HAMMER, CORROSION AND FATIGUE

NUREG-1061, Volume 3 [3] and GDC-4 [2] state that LBB should not be applied to high energy lines susceptible to failure from the effects of water hammer, corrosion or fatigue. These potential failure mechanisms are thus discussed below with regard to the RHR line at Ginna, and it is concluded that the above failure mechanisms do not invalidate the use of LBB for this piping system.

3.1 Water Hammer

A comprehensive study performed in NUREG-0927 [5] indicated that the probability of water hammer occurrence in the affected portions of the RHR system of a PWR is very low. In addition, RG&E has utilized EPRI guidelines and research results (References 30 and 31) to prevent, mitigate or accommodate water hammer events in Ginna systems.

3.2 Corrosion

Two corrosion damage mechanisms which can lead to rapid piping failure are intergranular stress corrosion cracking (IGSCC) in austenitic stainless steel pipes and flow-assisted corrosion (erosion-corrosion) in carbon steel pipes. IGSCC has principally been an issue in austenitic stainless steel piping in BWRs [6] resulting from a combination of tensile stresses, susceptible material and oxygenated environment. IGSCC is not typically a problem for the primary loop of a PWR such as the RHR system under consideration since the environment has relatively low concentrations of oxygen.

Erosion-corrosion is not anticipated to be a problem for this system since it is fabricated from stainless steel piping which is not susceptible to erosion-corrosion.



3.3 Fatigue

Known fatigue loadings and the resultant possible crack growth have been considered by the analyses reported in Section 6.0 of this report. Based on these results, it is concluded that fatigue will not be a significant issue for the RHR piping at Ginna.





4.0 PIPING MATERIALS AND STRESSES

4.1 Piping System Description

The mathematical models for the RHR piping system at Ginna are shown in Figures 1-1 through 1-3 [7,8]. The piping is fabricated from SA-376 Type 316 stainless steel. The welds are fabricated using either the submerged arc welding (SAW) or shielded metal arc welding (SMAW) processes. The lines are fabricated from 10-inch schedule 160 piping. The operating pressure for the RHR lines is 2235 psig and the operating temperature was conservatively chosen as 612.2°F to correspond to the temperature at which the RHR piping analysis was performed [32]. Use of the actual operating temperature of 550°F would yield larger critical flaw sizes and hence higher leakage rates.

4.2 Material Properties

The material properties used for the LBB evaluation are shown in Table 4-1. The elastic modulus (E), lower bound yield strength (σ_o) and ultimate strength (σ_u) are taken from the Appendices of Section III of the ASME Boiler and Pressure Vessel Code [10] at the operating temperature. The flow stress is computed as an average of the yield stress and ultimate stress, although this does not influence the crack stability results. The true stress-strain curve is represented by the Ramberg-Osgood power law equation in the form:

$$\varepsilon/\varepsilon_o = \sigma/\sigma_o + \alpha(\sigma/\sigma_o)^n$$

The Ramberg-Osgood true stress, true strain parameters, α and n , were obtained using the relationship from Reference 27 as:

$$n = \frac{1}{\ln(1+e_u)}$$



$$\alpha = \left[\frac{\ln(1+e_u)}{\ln(1+\sigma_y/E)} - \frac{\sigma_u(1+e_u)}{\sigma_y(1+\sigma_y/E)} \right] \left[\frac{\sigma_u(1+e_u)}{\sigma_y(1+\sigma_y/E)} \right]^{-n}$$

The J-integral versus crack extension (J-R) curves for flaw instability computations used in this evaluation represent the lower bound generic toughness values provided in the EPRI Ductile Fracture Handbook [9] for stainless steel weldments. For the critical flaw evaluations, the J-R curve is input in the form of a power law, as shown below:

$$J = C(\Delta a)^N$$

Δa = crack extension

The values for C and N obtained from Reference 9 are shown in Table 4-1.

4.3 Piping Stresses

The piping stresses which are normally considered in a LBB evaluation are due to pressure, dead weight, thermal expansion and Safe Shutdown Earthquake (SSE). Summaries of the pipe stresses for the RHR line are shown in Tables 4-2 and 4-3. These stresses are used to calculate the critical flaw size and the leakage rate through one-half the critical flaw size. For calculation of critical flaw size, the stress combination of pressure, deadweight, thermal and SSE loads is used. For leakage calculations, the stress combination of pressure, deadweight and thermal loads is used. These stress combinations are shown in Tables 4-2 and 4-3 for the various nodal locations. These piping stresses are listed by their piping model node numbers, which are shown in Figures 1-1 through 1-3. These node numbers, in general, correspond to the weld locations along the piping system. Stress intensification factors based upon B31.1 piping Code for the RHR piping [28] were calculated and extracted from the stresses obtained from the piping stress reports [7,8]. This is justified because for the fracture mechanics evaluation, it is the stress in the weld which is of interest, and not that in the adjacent component. The modified stresses excluding stress intensification factors are also shown in Tables 4-2 and 4-3.

Table 4-1

Material Constants Used for Type 316
Stainless Steel in LBB Evaluation

Property	Value
E (ksi)	25,240 (1)
σ_o (ksi) ($=\sigma_y$)	18.8 (1)
σ_u (ksi)	71.8 (1)
σ_{flow} (ksi)	45.282 (2)
α	0.776 (3)
n	3.81 (3)
J_{lc} (in-kip/in ²)	0.99 (4)
J_{max} (in-kip/in ²)	5.0 (5)
C	6.033 (4)
N	0.391 (4)

Notes:

- (1) Taken from Reference 10 at the operating temperature of the RHR system.
- (2) Average of σ_o and σ_u
- (3) Determined using the procedure in Ref. 27.
- (4) Taken from Reference 9.
- (5) Maximum value used in the analysis.



Table 4-2
Calculation of Stresses for RHR Pipe Run from Valve 700 to Hot Leg

Pipe Run from Valve 700 to Hot Leg																			
		Input Stresses ⁷ , psi			Calculated Stress, ksi														
					Intensified Stresses								Unintensified Stresses					Load Combination	
Node	Type	Deadweight (DW) + Pressure (P)	Therm al (TH) ²	DW+ P + SSE	P ¹	P ³	DW	TH	SSE	i	i*0.75 ⁶	P ^{1,9}	P ^{3,9}	DW	TH ⁸	SSE	P + DW+ TH + SSE	P + DW + TH	
680	30° Taper Transi- tion ⁴	6047	3121	18011	4.145	3.728	1.902	3.121	11.964	1.534	1.151	4.145	3.728	1.653	2.034	10.396	17.811	7.415	
50	Elbow ³	7030	1165	15997	4.145	3.728	2.885	1.165	8.967	1.111	1.000	4.145	3.728	2.885	1.048	8.967	16.628	7.661	
60	Elbow ³	6263	1719	15644	4.145	3.728	2.118	1.719	9.381	1.111	1.000	4.145	3.728	2.118	1.547	9.381	16.774	7.393	
70	30° Taper Transi- tion ⁵	6197	1397	15402	4.145	3.728	2.052	1.397	9.205	1.534	1.151	4.145	3.728	1.783	0.910	7.9019	14.420	6.422	

Notes:

1) Pressure Stress for Design Conditions (based upon pressure of 2485 psig); calculated with the following equation: $P \frac{D_o^2}{D_o^2 - D_i^2}$ where D_o = outer diameter = 10.75 and D_i = inner diameter = 8.5.

2) Thermal stress for Normal Operating Conditions.

3) Pressure Stress for Normal Operating Conditions (based upon pressure of 2235 psig); calculated with the following equation $P \frac{D_i^2}{D_o^2 - D_i^2}$.

4) Stress intensity factor i , calculated for 30° taper transition with the following equation: $i = 1.9 \text{ max or } i = 1.3 + 0.0036D_o/t + 0.225/t$ where $D_o = 10.75 \text{ in.}$ and $t = \text{thickness} = 1.125 \text{ in.}$

5) Stress intensity factor i , calculated for welding elbow with the following equation: $i = 0.9/h^{2/3} = 1.111$ where $h = TR/(r)^2 = 0.7286$; t = nominal wall thickness = 1.125 in., R = bend radius = 15 in., and r = mean radius = 4.8125 in.

6) $i \cdot 0.75$ cannot be < 1.

7) All input stresses taken from References 7 and 8.

8) For B31.1, thermal stresses do not include 0.75 multiplier.

9) For B31.1, pressure stresses do not include stress intensity factor, i .

Table 4-3
Calculation of Stresses for RHR Pipe Run from Valve 721 to Cold Leg

Pipe Run from Valve 721 to Cold Leg																				
		Input Stresses, psi			Calculated Stress, ksi															
					Intensified Stresses							Unintensified Stresses					Load Combination			
Node	Type	Deadweight (DW) + Pressure (P)	Thermal (TH) ²	DW+ P + SSE	P ¹	P ³	DW	TH	SSE	i	i*0.75 ⁶	P ^{1,9}	P ^{3,9}	DW	TH ⁸	SSE	P + DW+ TH + SSE	P + DW + TH		
8400	Weld-o-let ⁴	7794	9927	10154	4.145	3.728	3.649	9.927	2.360	1.534	1.151	4.145	3.728	3.171	6.470	2.051	15.419	13.368		
910	Elbow ⁵	6868	11560	9170	4.145	3.728	2.723	11.560	2.302	1.111	1.000	4.145	3.728	2.723	10.400	2.302	19.153	16.851		
920	Elbow ⁵	5416	8887	9050	4.145	3.728	1.271	8.887	3.634	1.111	1.000	4.145	3.728	1.271	7.996	3.634	16.629	12.995		
930	Elbow ⁵	5735	7066	8715	4.145	3.728	1.590	7.066	2.980	1.111	1.000	4.145	3.728	1.590	6.357	2.980	14.655	11.675		
950	Elbow ⁵	5417	5931	7740	4.145	3.728	1.272	5.931	2.323	1.111	1.000	4.145	3.728	1.272	5.336	2.323	12.659	10.336		
960	Weld-o-let ⁴	5209	7038	7451	4.145	3.728	1.064	7.038	2.242	1.534	1.151	4.145	3.728	0.924	4.587	1.948	11.188	9.239		

Notes:

- 1) Pressure Stress for Design Conditions (based upon pressure of 2485 psig); calculated with the following equation: $P \frac{D_i^2}{D_o^2 - D_i^2}$ where D_o = outer diameter = 10.75 and D_i = inner diameter = 8.5.
- 2) Thermal stress for Normal Operating Conditions.
- 3) Pressure Stress for Normal Operating Conditions (based upon pressure of 2235 psig); calculated with the following equation: $P \frac{D_i^2}{D_o^2 - D_i^2}$
- 4) Stress intensity factor i , calculated for 30° taper transition with the following equation: $i = 1.9 \text{ max or } i = 1.3 + 0.0036D_o/t + 0.225/t$ where D_o = outer diameter = 10.75 in. and t thickness = 1.125 in.
- 5) Stress intensity factor i , calculated for welding elbow with the following equation: $i = 0.9/h^{2/3} = 1.111$ where $h = TR/(r)^2 = 0.7286$; T = nominal wall thickness = 1.125 in., R = bend radius = 15 in., and r = mean radius = 4.8125 in.
- 6) $i \cdot 0.75$ cannot be <1.
- 7) All input stresses taken from References 7 and 8.
- 8) Per B31.1, thermal stresses do not include 0.75 multiplier.
- 9) Per B31.1, pressure stresses do not include stress intensity factor, i .

5.0 LEAK-BEFORE-BREAK EVALUATION

The LBB approach involves the determination of critical flow sizes, critical stresses and leakage through flaws. The critical flow length for a through-wall flaw is that length for which, under a given set of applied stresses, the flaw would become marginally unstable. Similarly, the critical stress is that stress at which a given flow size becomes marginally unstable. NUREG-1061, Volume 3 [3] defines required margins of safety on both flow length and applied stress. However, as explained in Section 2, safety margins based on flow length have been found in previous evaluations to be the more conservative of the two and therefore, only the criterion based on flow length will be used in this evaluation. Furthermore, previous evaluations [4] have demonstrated that circumferential flaws are more restrictive than postulated axial flaws. For this reason, the evaluation presented herein will be based on assumed circumferential flaws.

5.1 Evaluation of Critical Flow Sizes

Critical flow sizes may be determined using net section collapse criterion (NSCC) approach or J-Integral/Tearing Modulus (J/T) methodology. NSCC is particularly suited for materials with a considerable amount of ductility and toughness such as stainless steel materials, since it assumes that the cross-section of the pipe becomes fully plastified at the onset of failure. As such, for circumferential flaws, NSCC is less conservative compared to the J/T methodology which is based on elastic-plastic fracture mechanics (EPFM) principles. The conservatism in the use of EPFM was demonstrated on previous LBB evaluations for Ginna [4] and other similar evaluations performed by SI. In this evaluation, the critical flow sizes will therefore be determined based on the J/T approach.

A procedure for using this approach for the assessment of the stability of through-wall circumferential flaws in cylindrical geometries such as pipes is presented in References 11 and 12. This procedure was used for the determination of critical stresses and flow sizes in the RHR piping at Ginna, using SI's computer program, pc-CRACK™ [13].





The expression for the J-integral for a through-wall circumferential crack under tension loading [18] which is applied in this analysis is:

$$J = f_1 \left(a_c, \frac{R}{t} \right) \frac{P^2}{E} + \alpha \sigma_o \epsilon_o c \left(\frac{a}{b} \right) h_1 \left(\frac{a}{b}, n, \frac{R}{t} \right) \left[\frac{P}{P_o} \right]^{n+1}$$

where

$$f_1 \left(a_c, \frac{R}{t} \right) = \frac{a_c F^2 \left(\frac{a}{b}, \frac{R}{t} \right)}{4\pi R^2 t^2}$$

- a_c = effective crack length including small scale yielding correction
- R = nominal pipe radius
- t = pipe wall thickness
- F = elasticity factor [18,19]
- P = applied load = $\sigma_\infty \cdot 2\pi R t$; where σ_∞ is the remote tension stress in the uncracked section
- α = Ramberg-Osgood material coefficient
- E = elastic modulus
- σ_o = yield stress
- ϵ_o = yield strain
- c = $b-a$
- $2a$ = crack length
- $2b$ = $2\pi R$
- h_1 = plasticity factor [11, 12]
- P_o = limit load corresponding to a perfectly plastic material
- n = Ramberg-Osgood strain hardening exponent.

Similar equations [11, 12] are used to compute critical flaw sizes for circumferential TWCs under bending stresses. Crack extensions during stable ductile tearing in the EPFM analyses are

conservatively not included in the critical flaw length computations. The piping stresses consists of both tension and bending stresses. The tension stress is due to internal pressure while the bending stress is caused by deadweight, thermal and seismic loadings. The critical flaw sizes (lengths) obtained with the tension model (a_t) and the bending model (a_b) are combined to determine the actual critical flaw size (a_c) due to a combined tension and bending stress using linear interpolation, as described by the following equation:

$$a_c = a_t \frac{\sigma_t}{\sigma_b + \sigma_t} + a_b \frac{\sigma_b}{\sigma_b + \sigma_t}$$

The results of the critical flaw size determination are presented in Table 5-1.

5.2 Leak Rate Determination

The determination of leak rate is performed using the Structural Integrity Associates program, **pc-LEAK** [14]. The methodology employed in **pc-LEAK** involves the determination of crack opening area (COA), assuming plasticity at the crack tip. Then, the flow rate is determined based on classical thermal-hydraulic expressions for single and two-phase flow.

Crack opening area under the influence of steady-state operating stress (combined tension and bending) is computed from References 15 and 16 as:

$$A_c = \frac{\sigma_t}{E} (\pi R^2) I_t(\theta) \left[1 + \frac{\sigma_b}{\sigma_t} \left(\frac{3 + \cos \theta}{4} \right) \right]$$

where

- A_c = crack opening area (in^2) including plastic zone correction, assuming plane stress
- σ_t = steady-state tension stress (psi)
- σ_b = steady-state axial bending stress (psi)
- E = elastic modulus (psi)

- R = nominal pipe radius (in.), and
 θ = the angle describing half the through-wall crack length (radians).

The term $I_t(\theta)$ is computed for varying R/t (pipe radius/thickness) in accordance with the equations of Reference 16.

The plastic zone correction for the effect of yielding near the crack tip is incorporated by the following equation [15]:

$$\theta_e = \theta + \frac{K_{total}^2}{2\pi R \sigma_y^2}$$

where

- θ_e = effective half-length of angle through-wall crack, assuming plane stress
 K_{total} = stress intensity factor due to combined tension and bending
 σ_y = reference stress

In this evaluation, the flow stress which is the average of yield and ultimate strength was appropriately used as the reference stress.

The flow rate through the crack is based on classical thermal-hydraulic methodology. The development of the approach is detailed in the following section. The methodology includes considerations of both liquid and vapor flow of water, including the consideration of two phase flow within the crack.

The crack is considered to have a total length of 2a, either around the circumference or axially along the pipe wall. The crack has an average opening width w, and the flow path length through the wall is taken as L.

The hydraulic diameter [17] of a flow path is:

$$D_H = \frac{4A}{P}$$

where:

D_H = hydraulic diameter

A = cross sectional area

P = perimeter.

For a narrow crack of length $2a$,

$$D_H = \frac{4 \times A}{(2)(2a)} = \frac{A}{a}$$

If w is the average crack opening width, then

$$A = 2aw$$

and

$$D_H = 2w$$

The frictional loss in the constant area channel will be assumed to be that between parallel plates with a surface roughness. The parameter of interest to characterize the flow resistance per unit of area is:

$$K_{eff} + K_{exit} = \sum K_i + \frac{fL}{D_H} + K_{exit}$$

where:

K_{eff} = effective total pressure loss coefficient

K_i = individual discontinuity total pressure loss coefficient

f = friction factor

L = flow path length, (pipe wall thickness)

D_H = hydraulic diameter

K_{exit} = exit loss coefficient = 1.0.

The pressure loss coefficients for the entrance and flow direction changes must be computed separately from the friction loss parameters. For example, Reference 18 recommends a discontinuity loss coefficient of 0.5 for a sharp entrance crack with gaseous flow. Reference 19 recommends a value of 2.7 to properly account for the vena contracta (reduction in cross section) when dealing with near saturated water entering a narrow crack.

The friction factor for turbulent flow (Reynolds number > 4000) is determined from Reference 20:

$$\frac{1}{\sqrt{f}} = -2 \log_{10} \left(\frac{\epsilon}{3.7 D_H} + \frac{2.52}{Re \sqrt{f}} \right)$$

where:

- f = friction factor
- ϵ = surface roughness
- D_H = hydraulic diameter
- Re = Reynolds number.

For laminar flow between parallel plates, Reference 21 recommends:

$$f = \frac{96}{Re}$$

which occurs below about $Re = 2000$. In the transition range between $2000 < Re < 4000$, a best estimate friction factor is used.

In the turbulent equation, an iterative approach must be taken to solve for the friction factor. Iteration is also required to determine the friction factor in the transition regime of Reynolds number.

Reference 19 recommends a value of 5 μm (0.000197 inches) for the surface roughness of fatigue cracks. For more tortuous paths, and extremely small crack opening displacements, additional losses might be input with increased values for K. However, this effect will be quite small for crack opening widths which will produce detectable leakage in a power piping system.

For the pipe region filled with subcooled water, the flow can be determined by standard incompressible flow methodology. For saturated steam flow, the mass flow rate versus inlet total pressure may be determined directly from the charts of fL/D from Reference 22. Similarly, Reference 22 provides charts for the blowdown of water and steam-water mixtures. These are incorporated as tables in pc-LEAK [14].

In evaluating the flow of subcooled water, which flashes as the static pressure reaches saturation, a two-step approach is used. For the subcooled portion of the flow, the incompressible flow equation is used:

$$P_{T,inlet} - P_{sat} = (K_{inlet} + 1.0 + \frac{fL}{D_H}) \frac{1}{2} \rho V^2$$

where

- $P_{T,inlet}$ = pressure inside pipe
- P_{sat} = saturation pressure associated with water temperature in pipe
- ρ = liquid density
- V = velocity
- K_{inlet} = inlet plus discontinuity loss coefficient
- 1.0 = total to static pressure loss coefficient at the downstream end of the flow.

From this equation, the length (fL_1/D) of channel to bring fluid from its subcooled condition to a flashing saturated mixture may be determined as a function of mass flux. This is illustrated in Figure 5-1.

In length L_2 , a two-phase homogeneous mixture flows and this length may be determined for saturated water from the Reference 22 charts. For small values of fL_2/D , the saturation flashing point may occur just at the exit of the crack, such that the flow can be approximately determined solely based upon flow of liquid water. When the inlet pressure is near saturation pressure, the flow may be approximately determined from the Reference 22 charts. In between, a combined flow situation exists.





The leakage was calculated for an operating pressure of 2235 psig and a temperature of 612.2°F. Parametric evaluations showed that use of lower temperatures would produce higher leak rates. The leakage results are presented graphically in Figures 5-2 and 5-3 as a function of crack size (2a) for the various locations on the hot leg side, as well as the cold leg side. Table 5-2 shows the predicted leakage as a function of the critical flaw size for each location.

5.3 LBB Evaluation Results and Discussions

As can be seen from Table 5-2, the calculated leakage through half the critical flaw size for locations adjacent to the hot leg is at least 4.7 gpm considered in this evaluation. The leakage increases to at least 16.5 gpm at these locations if three-quarters of the critical flaw size is considered. Due to relatively high thermal stresses at the locations near the cold leg, the leakage through half the critical flaw size is relatively large (at least 13.4 gpm). This increases to at least 44.7 gpm when three-quarter the critical flaw size is considered. It is believed that the leakage through half the critical flaw size can be determined by the leak detection system at Ginna which is capable of measuring 1 gpm leakage [24].



Table 5-1

Summary of Critical Flaw Sizes

			Critical Flaw Length (2a), in.		
Node No.	Total Stress, ksi	Tension Stress, ksi	Tension	Bending	Combination
Hot Leg					
680	17.811	3.728	8.814	11.537	10.967
50	16.628	3.728	9.349	12.120	11.499
60	16.774	3.728	9.282	12.046	11.432
70	14.420	3.728	10.449	13.285	12.552
Cold Leg					
8400	15.419	3.728	9.934	12.745	12.065
910	19.153	3.728	8.249	10.908	10.390
920	16.629	3.728	9.349	12.120	11.498
930	14.655	3.728	10.325	13.156	12.436
950	12.659	3.728	11.437	14.299	13.456
960	11.188	3.728	12.672	15.200	14.358



Table 5-2

LBB Evaluation Results for Detectable Leakage

Node No.	Critical Flaw Length (2a) (in.)	Leakage at Fraction of Critical Flaw Length (gpm)		
		One-quarter	One-half	Three-quarter
Hot Leg				
680	10.967	0.60	4.71	16.5
50	11.499	0.73	5.74	20.2
60	11.432	0.67	5.31	18.8
70	12.552	0.69	5.64	21.2
Cold Leg				
8400	12.065	2.36	16.2	54.8
910	10.390	2.44	15.82	50.1
920	11.498	1.96	13.46	44.7
930	12.436	2.00	14.14	48.93
950	13.456	2.01	14.69	53.5
960	14.358	2.03	15.00	57.5



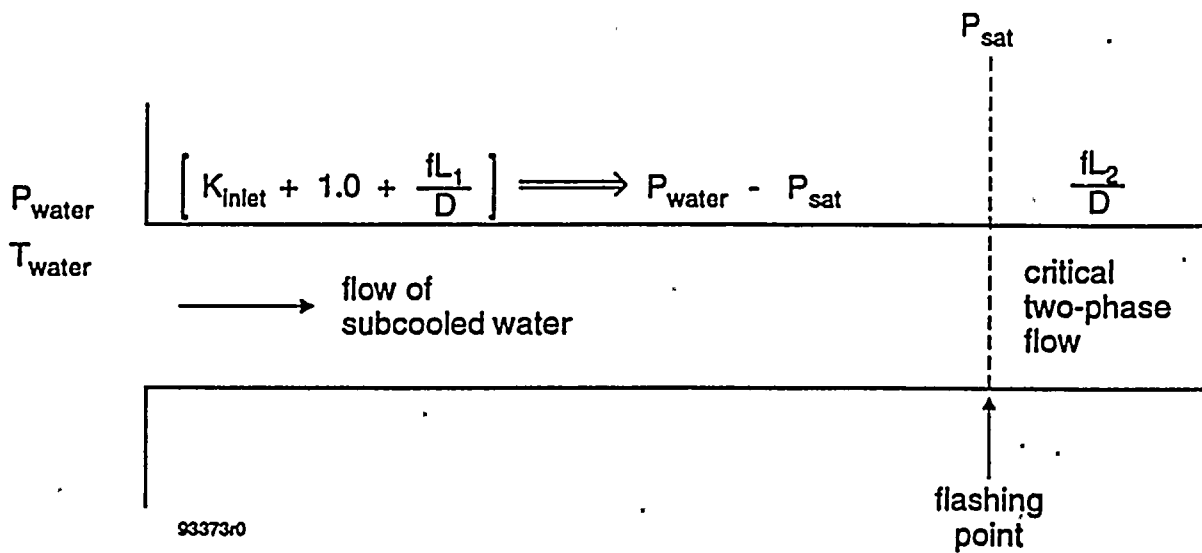


Figure 5-1. Flow of Subcooled Water Through a Crack



*Leakage Evaluation
Hot Leg*

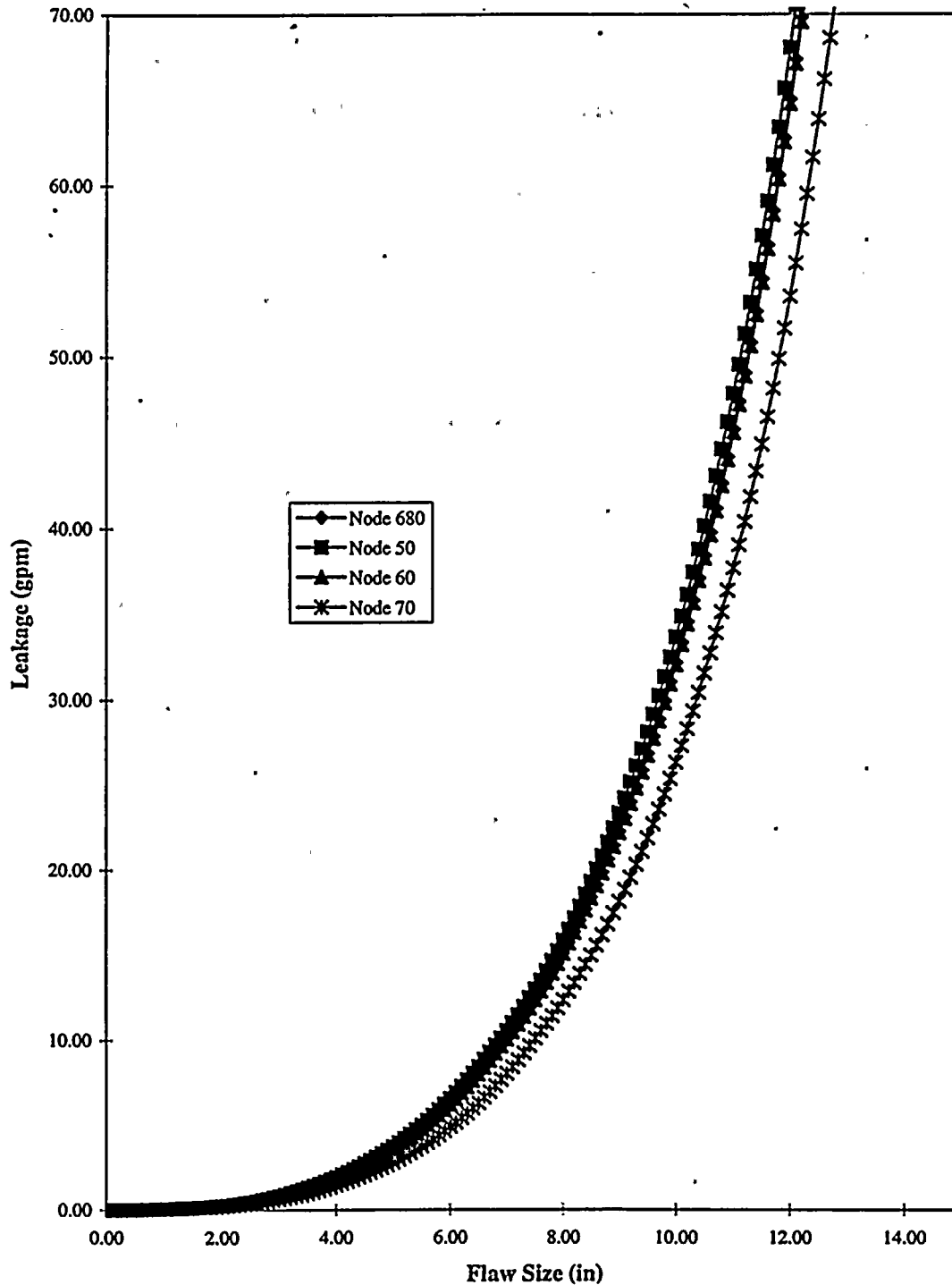


Figure 5-2. Leak Rate Versus Crack Length (2a) for RHR Pipe Run from Valve 700 to Hot Leg

*Leakage Evaluation
Cold Leg*

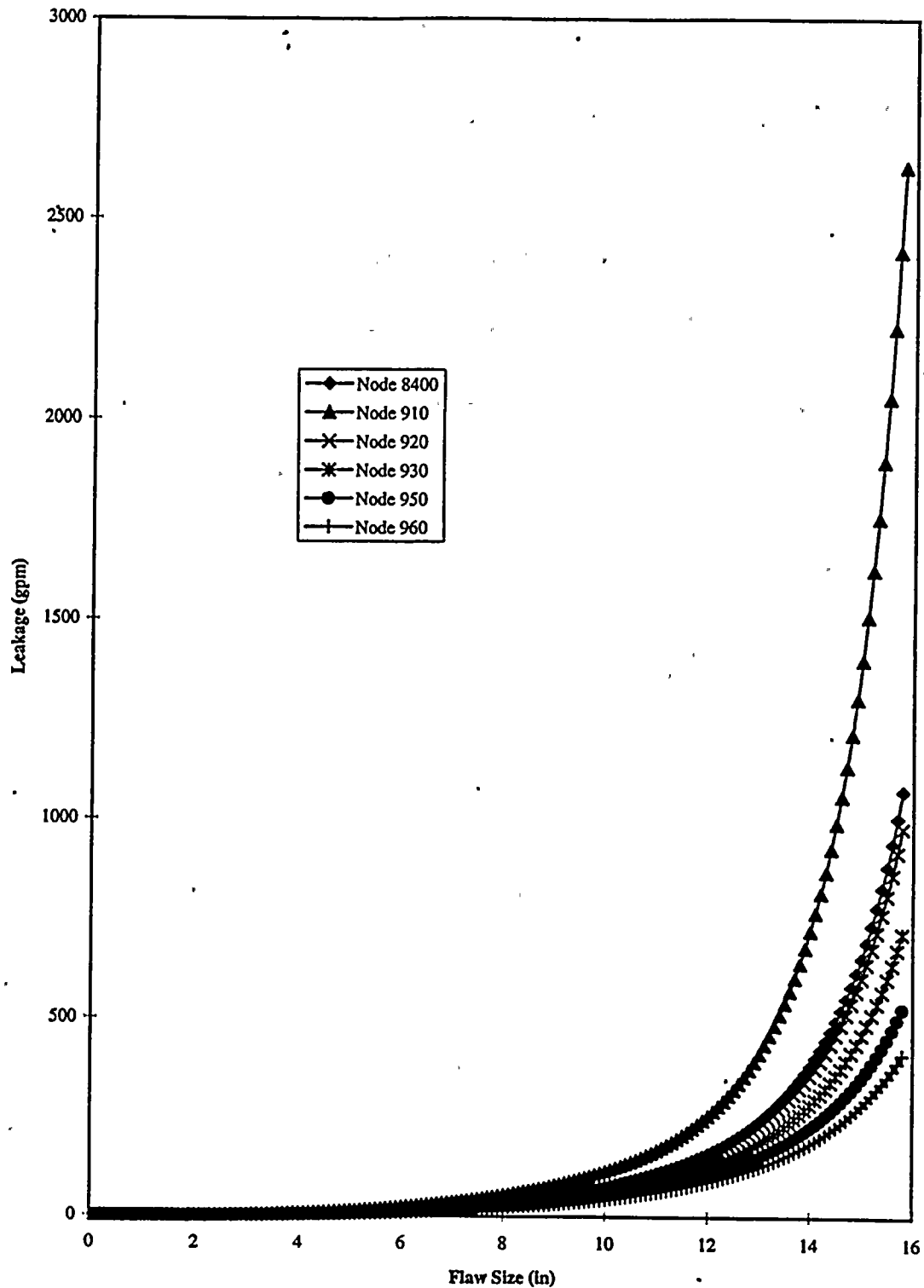


Figure 5-3. Leak Rate Versus Crack Length (2a) for RHR Pipe Run from Valve 721 to Cold Leg

6.0 EVALUATION OF FATIGUE CRACK GROWTH OF SURFACE FLAWS

In accordance with the NRC criteria [2,3] set forth in Section 2 of this report, the growth of postulated surface cracks by fatigue is evaluated to demonstrate that such growth is insignificant for the plant life, when initial flaw sizes in excess of those meeting ASME Code Section XI IWB-3514 are postulated. Furthermore, the growth of larger postulated initial flaws, in both depth and length directions, is studied to demonstrate that such flaws would tend to grow through the pipe wall (in the depth direction) to result in detectable leakage prior to significantly impacting safety margins by extending in length.

The stress intensity factors, K , corresponding to the point of the maximum depth of a semi-elliptical crack are calculated using pc-CRACK™ [13]. The K values are calculated for each pipe size for a reference 10 ksi uniform tension and pure bending stress. In each case, the stress intensity factors are determined for a conservative aspect ratio (a/ℓ) of 0.1. The stress intensity magnification factors derived in Reference 23 were used to compute the K value corresponding to the point of maximum length at the inside surface of the pipe.

Plant design transients for the RHR piping [24,25] are shown in Table 6-1. The normal operational mode of the RHR system is that it is used for decay heat removal during the latter portions of cooldown. At about 350°F, the RHR system is initiated. However, the plant procedures [33] require that the RHR system be pressurized and slowly warmed prior to use. This is accomplished by circulating flow through the RHR system into the letdown line. As a result, when return flow to the reactor coolant loop is initiated, there is no significant thermal transient. Therefore this transient is not considered in Table 6-1.

For the purpose of crack growth analysis, the transients shown in Table 6-1 are conservatively combined into fourteen (14) different load combinations based on their pressure and temperature ranges. The combined transients and associated number of cycles are shown in Tables 6-2 and 6-3.

The pressure and temperature values corresponding to these combined transients were used to linearly scale the pressure and thermal stresses corresponding to operating conditions. The axial



stresses due to the pressure and thermal differentials for each of the transient categories are calculated as follows:

For an applied pressure of P, the axial stress is calculated as:

$$\sigma_p = P \frac{D_i^2}{D_o^2 - D_i^2}$$

where D_o is the outside diameter and D_i is the inside diameter.

For thermal loads, ΔT , the stress is the maximum operating thermal stress, shown in Tables 4-2 and 4-3, factored by the ratio of the transient temperature to the operating temperature gradients:

$$\sigma_t = \sigma_{\max, \text{oper}} \frac{\Delta T}{\Delta T_{\text{oper}}}$$

The calculated axial pressure and thermal stresses are presented in Tables 6-4 and 6-5. Tables 6-4 and 6-5 also show the total stresses, including the deadweight stress for Nodes 680 and 910 shown in Tables 4-2 and 4-3.

Using the K results calculated above with **pc-CRACK™** [13] and the transients in Table 6-2, the fatigue crack growth law recommended in Ref. 25 for stainless steel in a PWR environment was employed to compute crack growth for various postulated initial flaw sizes. This crack growth is given by:

$$da / dN = C E S (\Delta K)^n$$

where

da/dN = change in crack depth, a, per fatigue cycle, in./cycle

C, n = material constants, $n = 3.3$, $C = 2 \times 10^{-19} \text{ (in./cycle)/(psi } \sqrt{\text{in}} \text{)}^n$



S	=	R ratio correction factor = $[1.0 - 0.5R^2]^{-4}$
R	=	K_{min}/K_{max}
E	=	environmental factor (equal to 1.0, 2.0, and 10.0 for air, PWR, and BWR environments, respectively)
ΔK	=	$K_{max} - K_{min}$, psi $\sqrt{\text{in}}$ and
K_{min}, K_{max}	=	minimum and maximum values, respectively, of applied stress intensity factor

A value of 2.0 was used for the parameter E in the above equation. Two bounding R ratios of 0.0 and 1.0 were used to calculate the crack growth. The R ratio of 0.0 corresponds to a case where the effect of residual stresses is minimal while an R ratio of 1.0 conservatively represents the case where residual stresses contribute significantly to the total stresses. In equivalent ksi units, the crack growth laws for these two R ratios can be written as:

$$da/dN = 3.177 \times 10^{-9} (\Delta K)^{3.3} \text{ for } R = 0.0$$

$$da/dN = 5.083 \times 10^{-8} (\Delta K)^{3.3} \text{ for } R = 1.0$$

The analysis is performed for Node point 910 of the cold leg RHR loop since this location has the maximum thermal stress range as can be seen from Table 4-3. The stresses are cycled between maximum and the minimum stresses shown in Table 6-5. The weld residual stress is conservatively represented by a pure through-wall bending stress equal to the pipe material (SA 376, Type 316 stainless steel) yield stress at the operating temperature of 612.2°F ($S_y = 18.8$ ksi). For each pipe size and enveloping transient category, the appropriate scaling factors, based upon a reference stress of 10 ksi and actual stress values given in Table 6-3, are input to obtain the actual K values for the fatigue crack growth.

For the crack growth in the depth direction, the analysis is performed for three initial crack depths ($a/t = 0.15, 0.5$ and 0.7). In the length direction, the calculations are performed for depth-to-wall thickness ratios ($a/t = 0.15, 0.6$ and 0.8). These ratios correspond approximately to the final a/t

ratios for crack growth in the depth direction after 40 years or when the crack reaches 80% of pipe thickness.

The fatigue crack growth analysis results are summarized in Table 6-6. It can be seen that postulated circumferential flaws 15% of pipe wall by about 0.84 inches long ($\ell/a = 10$) do not grow significantly in 40 years of plant operation. Evaluation of deeper postulated flaws (50% and greater) for both R ratios, shows that such cracks would grow through the pipe wall before extending significantly in length. In all cases, the crack would grow through-wall before extending in length more than 0.3 inches. Thus, detectable leakage would result before LBB safety margins are violated.



Table 6-1. Plant Design Transients for RHR Piping

Design Condition	Design Transients	Number of Cycles	ΔP (psi)	$\Delta T(1)$ (°F)
Level A	Plant Heatup/Cooldown	200	1935	447
	Plant Loading/Unloading	14,500	0	58/5
	10% Step Increase/Decrease	2,000	180	25/29
	Steady State Fluctuations	Infinite	100	6
Level B	Reactor Trip at Full Power	400	320	58/23
	Step Reduction 50% to 0%	400	100	13/16
	Loss of Power	40	250	103/58
	Loss of Load	80	1250	113/53
	Loss of Flow	80	340	92/37
Test	Primary Pressure Test	40	2485	300
	Primary Leakage Test	100	2250	200

(1) First number represents hot leg and second represents cold leg.

Table 6-2
Combined Transients For Fatigue Crack Growth Evaluation
for RHR Line Adjacent to Hot Leg

Hot Leg Cycles

Load Case	Load Combination Description	Block Cycles	P _{max} psig	P _{min} psig	T _{max} °F	T _{min} °F	ΔP, psi	ΔT, °F	Notes
1	Pressure Test	1	2485	0	547	70	2485	477	Max ΔT assumed
2	Leak Test	2.5 (1)	2250	0	547	70	2250	477	
3	Heatup/Cooldown + Loss of Load (Up)	2	2800	0	660	70	2800	590	
4	Heatup/Cooldown + Loss of Power (Up)	1	2500	0	650	70	2500	580	
5	Heatup/Cooldown + 50% Reduction (Up)	2	2350	0	605	70	2350	535	For T _{max} , use Plant Loading
6	50% Reduction (Up) + Loss of Power (Dn)	1	2350	1550	588	547	800	41	
7	50% Reduction (Up) + Loss of Load (Dn)	2	2350	1550	588	547	800	41	
8	50% Reduction (Up) + Loss of Flow (Dn)	2	2350	1910	588	520	440	68	
9	50% Reduction (Up) + Reactor Trip (Dn)	5	2350	1930	588	547	420	41	
10	10% Step Increase (Up) + Reactor Trip (Dn)	5	2330	1930	615	547	400	68	
11	10% Step Incr(Up) + 10% Step Decr (Dn)	45	2330	2150	615	592	180	23	
12	10% Step Decr (Up) + 10% Step Decr (Dn)	5	2290	2150	615	592	140	23	
13	10% Step Decr (Up) + 10% Step Incr (Dn)	45	2290	2150	615	590	140	25	
14	Remaining (Up) + Remaining (Dn)	377.5(2)	2250	2150	605	547	100	58	

- (1) For analysis purposes, 3 cycles are used.
(2) For analysis purposes, 378 cycles are used.





Table 6-3
Combined Transients For Fatigue Crack Growth Evaluation For
RHR Line Adjacent to Cold Leg

Cold Leg Cycles

Load Case	Load Combination Description	Block Cycles	P _{max} psig	P _{min} psig	T _{max} °F	T _{min} °F	ΔP, psi	ΔT, °F	Notes
1	Pressure Test	1	2485	0	547	70	2485	477	Max ΔT assumed
2	Leak Test	2.5(1)	2250	0	547	70	2250	477	Max ΔT assumed
3	Heatup/Cooldown + Loss of Load (Up)	2	2800	0	600	70	2800	530	
4	Heatup/Cooldown + Loss of Power (Up)	1	2500	0	600	70	2500	530	
5	Heatup/Cooldown + 50% Reduction (Up)	2	2350	0	582	70	2350	512	
6	50% Reduction (Up) + Loss of Power (Dn)	1	2350	1550	582	547	800	35	
7	50% Reduction (Up) + Loss of Load (Dn)	2	2350	1550	582	547	800	35	
8	50% Reduction (Up) + Loss of Flow (Dn)	2	2350	1910	582	520	440	62	
9	50% Reduction (Up) + Reactor Trip (Dn)	5	2350	1930	582	547	420	35	
10	10% Step Increase (Up) + Reactor Trip (Dn)	5	2330	1930	568	547	400	21	
11	10% Step Incr(Up) + 10% Step Decr (Dn)	45	2330	2150	568	539	180	29	
12	10% Step Decr (Up) + 10% Step Decr (Dn)	5	2290	2150	555	539	140	16	
13	10% Step Decr (Up) + 10% Step Incr (Dn)	45	2290	2150	555	551	140	4	
14	Remaining (Up) + Remaining (Dn)	377.5(2)	2250	2150	557	547	100	10	

- (1) For analysis purposes, 3 cycles are used.
(2) For analysis purposes, 378 cycles are used.



Table 6-4

Combined Maximum and Minimum Stresses for Fatigue
Growth Analysis for RHR Line Adjacent to Hot Leg

Load Combination	<i>Hot Leg Stress Ranges (1)</i>							
	<i>Maximum Stress, ksi</i>				<i>Minimum Stress, ksi</i>			
	P	Th	DW	Total	P	Th	DW	Total
1	4.145	1.789	1.653	7.588	0.000	0.000	1.653	1.653
2	3.753	1.789	1.653	7.196	0.000	0.000	1.653	1.653
3	4.671	1.988	1.653	8.312	0.000	0.000	1.653	1.653
4	4.170	1.988	1.653	7.812	0.000	0.000	1.653	1.653
5	3.920	1.921	1.653	7.494	0.000	0.000	1.653	1.653
6	3.920	1.921	1.653	7.494	2.586	1.789	1.653	6.028
7	3.920	1.921	1.653	7.494	2.586	1.789	1.653	6.028
8	3.920	1.921	1.653	7.494	3.186	1.688	1.653	6.527
9	3.920	1.921	1.653	7.494	3.219	1.789	1.653	6.662
10	3.887	1.868	1.653	7.408	3.219	1.789	1.653	6.662
11	3.887	1.868	1.653	7.408	3.586	1.759	1.653	6.999
12	3.820	1.819	1.653	7.292	3.586	1.759	1.653	6.999
13	3.820	1.819	1.653	7.292	3.586	1.804	1.653	7.044
14	3.753	1.827	1.653	7.233	3.586	1.789	1.653	7.029

(1) A through-wall bending weld residual stress equal to the yield stress was also applied.



Table 6-5

Combined Maximum and Minimum Stresses for Fatigue Crack
Growth Analysis for RHR Line Adjacent to Cold Leg

<i>Cold Leg Stress Ranges (1)</i>								
Load Combination	<i>Maximum Stress, ksi</i>				<i>Minimum Stress, ksi</i>			
	P	Th	DW	Total	P	Th	DW	Total
1	4.145	9.149	2.723	16.018	0.000	0.000	2.723	2.723
2	3.753	9.149	2.723	15.626	0.000	0.000	2.723	2.723
3	4.671	10.166	2.723	17.560	0.000	0.000	2.723	2.723
4	4.170	10.166	2.723	17.059	0.000	0.000	2.723	2.723
5	3.920	9.821	2.723	16.464	0.000	0.000	2.723	2.723
6	3.920	9.821	2.723	16.464	2.586	9.149	2.723	14.458
7	3.920	9.821	2.723	16.464	2.586	9.149	2.723	14.458
8	3.920	9.821	2.723	16.464	3.186	8.632	2.723	14.541
9	3.920	9.821	2.723	16.464	3.219	9.149	2.723	15.092
10	3.887	9.552	2.723	16.162	3.219	9.149	2.723	15.092
11	3.887	9.552	2.723	16.162	3.586	8.996	2.723	15.305
12	3.820	9.303	2.723	15.846	3.586	8.996	2.723	15.305
13	3.820	9.303	2.723	15.846	3.586	9.226	2.723	15.536
14	3.753	9.341	2.723	15.817	3.586	9.149	2.723	15.459

(1) A through-wall bending weld residual stress equal to the yield stress was also applied.



Table 6-6. Results of Fatigue Crack Growth

R ratio	Assumed Initial a/t	Assumed Initial Depth (in.)	Final Depth (in.)	Final a/t	Assumed Initial Length (in.)	Final Length (in.)	Change in Length (in.)
0.0	0.15	0.16875	0.1719	0.1528	0.84375	0.8441	0.00035
	0.50	0.5625	0.6275	0.5563	3.3750	3.3822	0.00720
	0.70	0.7875	0.9005	0.8000	4.500	4.5146	0.01460
1.0	0.15	0.16875	0.2358	0.02096	0.84375	0.8490	0.00525
	0.50	0.5625	0.9061	0.800	3.3750	3.4893	0.1143
	0.70	0.7875	0.9177	0.800	4.500	4.7479	0.2479



7.0 SUMMARY AND CONCLUSIONS

Leak-before-break (LBB) evaluations are performed for the RHR system at R. E. Ginna in accordance with the requirements of NUREG-1061. In the evaluations, circumferential flaws are considered since they are more limiting than axial flaws. Critical flaw sizes and leakage rates through half the critical flaw sizes are calculated on a location specific basis for the RHR line at Ginna. Fatigue crack growth analysis was also performed to determine the extent of growth of any pre-existing flaws.

Based on these evaluations, the following conclusions can be made.

- Predicted leakage through half the critical flaw size for the RHR line adjacent to the hot leg is at least 4.7 gpm.
- Predicted leakage through half the critical flaw size for the RHR line adjacent to the cold leg is at least 16.2 gpm.
- Fatigue crack growth of subsurface flaws is insignificantly small and therefore does not invalidate the leak-before evaluation of the RHR lines.
- Based on the fact that the leak detection system at Ginna is capable of detecting 1 gpm leakage, leak-before-break has been demonstrated for the RHR line locations considered in this evaluation.



8.0 REFERENCES

1. Rochester Gas & Electric Corporation Drawings:
 - a) C-381-354 Sht. 1
 - b) C-381-354 Sht. 3
 - c) C-381-355 Sht. 8
2. Stello, Jr., V., "Final Broad Scope Rule to Modify General Design Criterion 4 of Appendix A, 10 CFR Part 50", NRC SECY-87-213, Rulemaking Issue (Affirmation), August 21, 1987.
3. NUREG-1061, Volumes 1-5, "Report of the U. S. Nuclear Regulatory Commission Piping Review Committee", prepared by the Piping Review Committee, NRC, April 1985.
4. Structural Integrity Associates Report No. SIR-85-034, Revision No. 1, "Fracture Mechanics Leak-Before-Break Evaluation of R. E. Ginna Nuclear Power Station High-Energy Piping Welds Outside Containment".
5. NUREG-0927, "Evaluation of Water Hammer Occurrence in Nuclear Power Plants" Revision 1.
6. W. S. Hazelton, W. H. Koo, "Technical Report on Material Selection and Processing Guidelines for BWR Coolant pressure Boundary Piping", NUREG-0313, Rev. 2, USNRC, January 1988.
7. Westinghouse Stress Report, SDTAR-80-05-05, Rev. 1, RHR 2500, dated 3/4/81.
8. Westinghouse Stress Report, SDTAR-80-05-26, SI-200 dated 3/20/81.
9. EPRI Report No. NP-6301-D "Ductile Fracture Handbook", June 1989.
10. ASME Boiler and Pressure Vessel Code, Section III, Division 1, 1989 Edition.
11. Kumar, V., et al., "Advances in Elastic-Plastic Fracture Analysis," EPRI NP-3607, August 1984.
12. Kumar, V., et al., "An Engineering Approach for Elastic-Plastic Fracture Analysis," EPRI NP-1931, July 1981.
13. Structural Integrity Associates, Inc., "pc-CRACK™ Fracture Mechanics Software", Version 3.0 - 3/27/97.





14. "pc-LEAK Calculation of Leakage Rates From Through-Wall Cracks", Version 1.0, Structural Integrity Associates, September 1996.
15. P. C. Paris, and H. Tada, "The Application of Fracture Proof Design Methods Using Tearing Instability Theory to Nuclear Piping Postulating Circumferential Through-Wall Cracks", NUREG/CR-3464, September 1983.
16. R. Klecker, F. Brust, and G. Wilkowski, "NRC Leak-Before-Break (LBB.NRC) Analysis Method for Circumferentially Through-Wall Cracked Pipes Under Axial Plus Bending Loads", NUREG/CR-4572, BMI-2134, May 1986.
17. Rohsenow and Choi, "Heat, Mass, and Momentum Transfer", Prentiss-Hall, New Jersey, 1961.
18. SAE Applied Aerospace Manual, Section I, "Engineering Fundamentals - Part A, Incompressible Fluid Flow".
19. EPRI Report NP-3395, "Calculation of Leak Rates Through Cracks in Pipes and Tubes", Electric Power Research Institute, December 1983.
20. "Marks Standard Handbook for Mechanical Engineers," Eighth Edition, McGraw Hill, New York, 1978.
21. R. D. Blevins, "Applied Fluids Dynamics Handbook", Van Nostrand Reinhold Co., New York, 1984.
22. R. J. Lahey, and F. J. Moody, "Thermal Hydraulics of Boiling Water Reactors", American Nuclear Society, 1977.
23. Huget, W. and Esser, K., "Stress Intensity Factors for Slender Surface Cracks", SMiRT Conference, Paper G/F 3/4, Chicago, 1983.
24. Ginna UFSAR, Table 5/1-4, Rev. 13 dated 12/96.
25. BWI Report No. 222-7705-SR-2, "Transient Analysis of Tubesheet/Primary Head and Secondary Shell Assembly", Section 2.1, October 2, 1995.
26. ASME Section XI Task Group for Piping Flaw Evaluation, "Evaluation of Flaws in Austenitic Steel Piping", Journal of Pressure Vessel Technology, Vol. 108, August 1986, pp.352-366.
27. EPRI Report NP-5531, "Evaluation of High-Energy Pipe Rupture Experiments", January 1988.



28. American National Standard, Power Piping, ANSI B31.1, 1973 Edition with Summer Addenda.
29. RG&E Action Report No. 97-1235, 8/14/97.
30. EPRI Report, TR-106438, 2856-02, "Water Hammer Handbook For Nuclear Plant Engineers And Operators", May 1996.
31. RG&E Action Reports 97-0404 & 0405.
32. Westinghouse Electric Corp. Letter No. PT-PQ-1584 from P.S. Van Teslaar to J. C. Hutton (RG&E), "R.E. Ginna Seismic Upgrading Program - Operating Transients Document Revision", June 11, 1982.
33. RG&E Procedure O-2.2, "Plant Shutdown From Hot Shutdown to Cold Conditions", Rev. 111, 10/21/96.



ROCHESTER GAS AND ELECTRIC CORPORATION

INTER-OFFICE CORRESPONDENCE

October 15, 1997

To: File

Subject: Evaluation of Structural Integrity Associates, Inc. Report
No. SIR-97-077

References: 1. RG&E Procedure, EP-3-P-154, "Review & Approval Of Vendor Drawings, Design And Manufacturing Technical Documents", Rev. 0.
2. Structural Integrity Associates (SIA), Inc. Report No. SIR-97-077, "Leak-Before-Break Evaluation of Portions of the Residual Heat Removal (RHR) System at R. E. Ginna Nuclear Power Station", Rev. 0.

Per RG&E Procedure in Reference 1, I reviewed the subject report (Reference 2) for technical correctness, relevance, and applicability to Ginna Nuclear Power Station. Method of review consisted of independent verification of fundamental concepts and criteria of the leak-before-break approach, input data, material properties, applicable loadings, effects of fluid/structure interaction on leakage quantification, and interpretation of results. In addition, I also discussed technical issues that were brought up by SIA independent reviewer and made sure these are resolved considering the existing RHR design basis, system requirements, transient operating conditions, and operating procedures.

Results of the review and evaluation are summarized below.

1. SIA has incorporated all RG&E comments in the final report.
2. Ginna plant specific input data, effects of procedural evolutions, technical programs, guidelines and regulatory commitments that were utilized in the leak-before-break study have been reviewed and confirmed per SIA QA program. No findings were discovered.
3. The leak-before-break methodology in the evaluation of the RHR piping is based on sound fundamental engineering concepts utilizing EPFM (elastic-plastic fracture mechanics) approach for calculating critical flaw sizes and classical thermal-hydraulic equations for evaluating single and two-phase flow. The approach is in accordance with Generic Design Criterion (GDC) 4 and NUREG-1061.
4. Results of leak-before-break evaluation (Reference 2) is applicable to Ginna due to the following factors:
 - a. Predicted minimum leakage of 4.7 gpm of the RHR line exceeds the minimum

leak detection capabilities of Ginna inside containment.

b. Other degradation mechanisms affecting the RHR piping such as water hammer, fatigue, erosion/corrosion, etc.. have negligible impact on the structural integrity of the RHR pipe.

5. Subject report is therefore acceptable to RG&E. It provides a technical basis that pipe rupture of the RHR pipe sections from the hot and cold legs of the reactor coolant system to MOV's 700 and 721 will not occur.

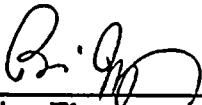
The leak-before-break report (Reference.2), in accordance with requirements of GDC 4 can be submitted to the NRC as a basis for showing that dynamic effects of pipe rupture of the evaluated RHR pipe sections has a negligible probability of occurrence.

Prepared by:



A. P. Rochino
Primary Systems Engineer

Approved by:



Brian Flynn
Manager, Primary Systems

cc: George Wrobel



Structural Integrity Associates, Inc.

September 23, 1997
NGC-97-040

3315 Almaden Expressway
Suite 24
San Jose, CA 95118-1557
Phone: 408-978-8200
Fax: 408-978-8964
ncofic@structint.com


Dr. Lee Rochino
Rochester Gas & Electric Company
R. E. Ginna Nuclear Power Station
1503 Lake Road
Ontario, NY 14519

Subject: Structural Integrity Associates Report No. SIR-97-077, Rev. 0, "Leak-Before-Break Evaluations of Portions of the Residual Heat Removal (RHR) System at R. E. Ginna Nuclear Power Station".

Dear Lee,

Enclosed are two bound copies and one unbound copy of the subject report for your use. We appreciate the opportunity to be of service to RG&E and you on this project. Please do not hesitate to call if you have any questions or comments.

Very truly yours,


Nathaniel G. Cofie, Ph.D.
Associate

sjl
enclosure

cc: G. Wrobel (RG&E)
RGE-07Q-102